Coupling Between Finite Elements and Boundary Elements for the Numerical Simulation of Induction Heating Processes Using a Harmonic Balance Method

Romain Pascal, Philippe Conraux, and Jean-Michel Bergheau

***Abstract*—For the modeling of induction heating processes, strongly coupled magnetodynamic and thermal problems can be solved together within the same finite element. This is called the direct method. In this case, the electromagnetic quantities are expressed through Fourier series according to the harmonic balance method. In this paper, each harmonic is calculated in the whole space by using the coupling between finite elements and boundary elements. Especially suitable when moving parts are involved and because the mesh of air is unnecessary, it is shown that this coupling is still successful if the direct method is used. At the end, the efficiency of this approach is illustrated with an example.**

***Index Terms*—FEM-BEM coupling, harmonic balance, induction heating, numerical simulation, strong coupling.**

I. Introduction

THE numerical simulation of induction heating rests on the modeling of both magnetodynamic and thermal nonlinear phenomena. These phenomena are strongly coupled because of the temperature dependency of the electric conductivity and nonlinear magnetization curves and the heat source due to Joule effect. Time constants associated with magnetodynamic and thermal phenomena differ considerably. Then, transient simulations for each problem are performed alternatively. The strong physical coupling is achieved with several loops back between both analyses at each thermal time step. Unfortunately, such a staggered method is very time consuming.

The direct method has been introduced in [1]. In this paper, magnetodynamic problem is solved considering only one harmonic of the electromagnetic unknowns and a modified magnetization curve [2]. The alternative method proposed in [3] is to take into account several harmonics according to the harmonic balance method [4]. In [5], comparisons between staggered and direct methods lead to the conclusion that a good compromise between time consumption and accuracy of results can be obtained.

In this paper, we deal with the numerical coupling between finite- and boundary-element methods (FEM and BEM) to solve the magnetodynamic problem in the whole space, each one combined with the harmonic balance method. This coupling technique is especially useful for the modeling of unmeshed air between moving parts involved in heating processes [6].

This paper is divided into four main parts: magnetodynamic analysis, thermal analysis, direct method, and application example.

Manuscript received June 18, 2002.

R. Pascal is with the Laboratoire de Tribologie et Dynamique des Systemes, LTDS, UMR5513 CNRS/ECL/ENISE, 42023 SAINT-ETIENNE Cedex 2, France, and also with the ESI SOFTWARE, 69485 LYON Cedex 03, France (e-mail: romain.pascal@enise.fr).

P. Conraux is with the ESI SOFTWARE, 69485 LYON Cedex 03, France (e-mail: philippe.conraux@esi-group.com).

J.-M. Bergheau is with the Laboratoire de Tribologie et Dynamique des Systemes, LTDS, UMR5513 CNRS/ECL/ENISE, 42023 SAINT-ETIENNE Cedex 2, France (e-mail: bergheau@enise.fr).

Digital Object Identifier 10.1109/TMAG.2003.810430

II. Magnetodynamic Analysis

A. Magnetodynamic Problem Solved With the Harmonic Balance Method

Even if the source currents are perfectly sinusoidal, the induced field inside the piece contains other higher harmonics due to the nonlinear electromagnetic properties. Instead of performing a transient analysis, the harmonic balance method can be used. This method consists in calculating the first terms of Fourier series of the different electromagnetic quantities as follows: $\mathbf{X}(\mathbf{x},t) = \sum_{k=1,3,\ldots}^{m}(\mathbf{X}_{kc}(\mathbf{x})\cos(k\omega t)+\mathbf{X}_{ks}(\mathbf{x})\sin(k\omega t))$ where ω is the fundamental angular frequency that is the angular frequency of the source currents.

From Maxwell's equations, neglecting displacement currents and introducing the magnetic vector potential $\mathbf{A}$, the magnetodynamic problem can be written as follows:

$$\sigma\frac{\partial \mathbf{A}}{\partial t} + \mathbf{rot}(\nu\,.\,\mathbf{rot}\,\mathbf{A}) - \mathbf{J_0} = 0 \quad \text{with div}\,\mathbf{A} = 0 \qquad (1)$$

where σ is the electric conductivity, ν the magnetic reluctivity, and $\mathbf{J_0}$ the source current density.

For an axisymmetrical geometry around an axis $\mathbf{e}_z$, the source current density $\mathbf{J_0}(\mathbf{x},t) = J_0(r,z,t)\,\mathbf{e}_\theta$ and the magnetic vector potential $\mathbf{A}(\mathbf{x},t) = A(r,z,t)\,\mathbf{e}_\theta$ present only one nonzero component depending on radial and axial coordinates. In this case, the second equation in (1) is automatically satisfied and first the equation in (1) only has to be solved in direction $\mathbf{e}_\theta$.

By using the harmonic balance, (1) is now replaced by the following equations, with $l = 1, 3, \ldots, m$:

$$\frac{2}{T}\int_0^T \left(\sigma\frac{\partial \mathbf{A}}{\partial t} + \mathbf{rot}(\nu\,.\,\mathbf{rot}\,\mathbf{A}) - \mathbf{J_0}\right).\cos(l\omega t)dt = 0 \qquad (2)$$

$$\frac{2}{T}\int_0^T \left(\sigma\frac{\partial \mathbf{A}}{\partial t} + \mathbf{rot}(\nu\,.\,\mathbf{rot}\,\mathbf{A}) - \mathbf{J_0}\right).\sin(l\omega t)dt = 0 \qquad (3)$$

B. Harmonic Balance and Boundary-Element Methods

The method coupling finite elements in the nonlinear conductive media and boundary elements in air has been successfully applied in [6] for induction heating simulation. By the way, the electromagnetic problem is perfectly solved in the whole space without any mesh of air. This approach is particularly well suited when moving parts are involved.

We assume that the whole space is subdivided into conductive regions Ω_{FEM}, possibly containing source currents, and air region Ω_{BEM}, free of any source current. $\Gamma_{\mathrm{FEM\text{-}BEM}}$ represents the common FEM-BEM boundary, and $\mathbf{n}_{\mathrm{FEM}}$ and $\mathbf{n}_{\mathrm{BEM}} = -\mathbf{n}_{\mathrm{FEM}}$ are the unit outside normals to $\Gamma_{\mathrm{FEM\text{-}BEM}}$ from Ω_{FEM} and Ω_{BEM} respectively.

In Ω_{BEM}, $\mathbf{A}(\mathbf{x},t)$ is the solution to the following equation:

$$\Delta\mathbf{A}(\mathrm{x},t) = 0 \tag{4}$$

with boundary conditions

$$\mathbf{A} = 0 \quad \text{to infinity } (\Gamma_\infty) \tag{5}$$

$$\text{Continuity to } \mathbf{A} \text{ and div } \mathbf{A} \text{ on } \Gamma_{\mathrm{FEM\text{-}BEM}} \tag{6}$$

$$\mathbf{Q} = \mathbf{H}\times\mathbf{n}_{\mathrm{FEM}} = -\mathbf{H}\times\mathbf{n}_{\mathrm{BEM}} \text{ on } \Gamma_{\mathrm{FEM\text{-}BEM}}. \tag{7}$$

The vector Laplace equation with boundary conditions has to be solved for each sine and cosine part of the $(m+1)/2$ harmonics of the magnetic vector potential. Therefore, it leads to the resolution of the following equations for $l = 1,3,\ldots,m$:

$$\Delta\left(A_{lc}(\mathbf{x})\mathbf{e}_\theta\right) = 0 \quad \text{and} \quad \Delta\left(A_{ls}(\mathbf{x})\mathbf{e}_\theta\right) = 0 \tag{8}$$

where A_{lc} and A_{ls} represent the cosine and sine parts of the harmonic of order l.

Both equations in (8) give rise to the following boundary-element equations:

$$[\mathbf{H}]\{\mathbf{A}_{lc,\mathrm{BEM}}\} - [\mathbf{G}]\{\mathbf{Q}_{lc,\mathrm{BEM}}\} = 0 \tag{9}$$

$$[\mathbf{H}]\{\mathbf{A}_{ls,\mathrm{BEM}}\} - [\mathbf{G}]\{\mathbf{Q}_{ls,\mathrm{BEM}}\} = 0 \tag{10}$$

where $\{\mathbf{A}_{lp,\mathrm{BEM}}\}$ ($p = c$ for the cosine part and $p = s$ for the sine part) is the unknown vector containing the nodal value of the part p of the harmonic l of the magnetic vector potential in Ω_{BEM}. In the same way, $\{\mathbf{Q}_{lp,\mathrm{BEM}}\}$ corresponds to the electromagnetic variable defined in (7). Refer to [6] to get matrices $[\mathbf{H}]$ and $[\mathbf{G}]$.

C. Coupling Between FEM and BEM

Let us consider a mesh of Ω_{FEM} (n nodes) and a compatible mesh of $\Gamma_{\mathrm{FEM\text{-}BEM}}$ (b nodes). The whole space Ω_{FEM} is subdivided in elements Ω^e. All elements are connected between them with nodes. In each element Ω^e, the spatial approximation of $A_{kp}(\mathbf{x})$ is the following:

$$\mathbf{x}\in\Omega^e,\ A_{kp}(\mathbf{x}) = \sum_{i=1}^{n^e} N_i^e A_{i,kp} = [\mathbf{N}^e]\cdot\left\{\mathbf{A}_{kp}^e\right\} \tag{11}$$

where n^e represents the number of nodes connected to element e, $\mathbf{A}_{i,kp}$ the unknown value at node i of element e, and N_i^e the shape function associated with node i of element e.

Equations (2) and (3) give rise to the resolution of the following equations for $l = 1,3,\ldots,m$:

$$\{\mathbf{R}_{lc}(\{A_{1c}\},\{A_{1s}\},\ldots)\} = \underset{e=1}{\overset{m}{\mathbf{A}}}\left\{\mathbf{R}_{lc}^e(\{\mathbf{A}_{1c}^e\},\{\mathbf{A}_{1s}^e\},\ldots)\right\} = 0 \tag{12}$$

$$\{\mathbf{R}_{ls}(\{A_{1c}\},\{A_{1s}\},\ldots)\} = \underset{e=1}{\overset{m}{\mathbf{A}}}\left\{\mathbf{R}_{ls}^e(\{\mathbf{A}_{1c}^e\},\{\mathbf{A}_{1s}^e\},\ldots)\right\} = 0. \tag{13}$$

Each of the $m+1$ residual vectors $\{\mathbf{R}_{lp}(\ldots)\}$ has n components. The total number of degrees of freedom is then equal to $(m+1)*n$ in this problem. Residual vectors are obtained through assembling the element residual vectors given at the bottom of the page, with for example

$$[\nu_{lc,ks}] = \frac{2}{T}\int_0^T \left[\nu\left(\|\mathbf{rot}\,\mathbf{A}\|\right)\right].\cos(l\omega t).\sin(k\omega t)dt. \tag{16}$$

Since compatible meshes are used for Ω_{FEM} and $\Gamma_{\mathrm{FEM\text{-}BEM}}$, the conditions defined in 6 are automatically fulfilled. Moreover, $\{\mathbf{A}_{lp,\mathrm{BEM}}\}$ is now a subset of $\{\mathbf{A}_{lp}\}$ limited to the nodes

---

$$\{\mathbf{R}_{lc}^e(\ldots)\} = -\int_{\Omega^e}[\mathbf{N}^e]^T.l\sigma\omega.[\mathbf{N}^e].\{\mathbf{A}_{ls}^e\}\,dv + \int_{\Omega^e}[\mathbf{N}^e]^T.\mathbf{J}_{0_{lc}^e}(\mathbf{x})dv - \sum_{k=1,3}^{m}\left(\int_{\Omega^e}[\mathbf{rot}\,\mathbf{N}^e]^T.[\nu_{lc,kc}].[\mathbf{rot}\,\mathbf{N}^e].\{\mathbf{A}_{kc}^e\}\,dv\right)$$
$$-\sum_{k=1,3}^{m}\left(\int_{\Omega^e}[\mathbf{rot}\,\mathbf{N}^e]^T.[\nu_{lc,ks}].[\mathbf{rot}\,\mathbf{N}^e].\{\mathbf{A}_{ks}^e\}\,dv\right) + \int_{\partial\Omega^e\cap\partial\Omega_{\Gamma_{\mathrm{FEM\text{-}BEM}}}}[\mathbf{N}^e]^T.\mathbf{Q}_{lc}^e(\mathbf{x})ds \tag{14}$$

and

$$\{\mathbf{R}_{ls}^e(\ldots)\} = +\int_{\Omega^e}[\mathbf{N}^e]^T.l\sigma\omega.[\mathbf{N}^e].\{\mathbf{A}_{lc}^e\}\,dv + \int_{\Omega^e}[\mathbf{N}^e]^T.\mathbf{J}_{0_{ls}^e}(\mathbf{x})dv - \sum_{k=1,3}^{m}\left(\int_{\Omega^e}[\mathbf{rot}\,\mathbf{N}^e]^T.[\nu_{ls,kc}].[\mathbf{rot}\,\mathbf{N}^e].\{\mathbf{A}_{kc}^e\}\,dv\right)$$
$$-\sum_{k=1,3}^{m}\left(\int_{\Omega^e}[\mathbf{rot}\,\mathbf{N}^e]^T.[\nu_{ls,ks}].[\mathbf{rot}\,\mathbf{N}^e].\{\mathbf{A}_{ks}^e\}\,dv\right) + \int_{\partial\Omega^e\cap\partial\Omega_{\Gamma_{\mathrm{FEM\text{-}BEM}}}}[\mathbf{N}^e]^T.\mathbf{Q}_{ls}^e(\mathbf{x})ds \tag{15}$$

belonging to $\Gamma_{\text{FEM-BEM}}$. Let us now suppose that the term $\mathbf{Q}_{lp}^{e}$ is defined from nodal values contained in a vector $\{\mathbf{Q}_{lp,\text{FEM}}\}$ (b components) by using shape functions of the elements lying on the boundary of Ω_{FEM}. Then, equation (7) leads to the following relation:

$$\{\mathbf{Q}_{lp,\text{FEM}}\} = -\{\mathbf{Q}_{lp,\text{BEM}}\}. \tag{17}$$

By considering the vectors: $\int_{\partial\Omega^e \cap \partial\Omega_{\Gamma_{\text{FEM-BEM}}}} [\mathbf{N}^e]^T.\mathbf{Q}_{lp}^{e}(\mathbf{x})\, ds$ we obtain the following vector:

$$[\mathbf{T}]\{\mathbf{Q}_{lp,\text{FEM}}\}. \tag{18}$$

Matrix $[\mathbf{T}]$ is obtained by assembling the element quantities: $\int_{\partial\Omega^e \cap \partial\Omega_{\Gamma_{\text{FEM-BEM}}}} [\mathbf{N}^e]^T.[\mathbf{N}^e]\ ds$. The vector (18) can then be replaced by the following one: $[\mathbf{T}].[\mathbf{G}]^{-1}.[\mathbf{H}]\{\mathbf{A}_{lp,\text{BEM}}\}$ thanks to (17) and (9) or (10). This matrix term represents the contribution of air to the resolution of magnetodynamic nonlinear problem by using the FEM inside conductive media.

III. Thermal Analysis

For the thermal analysis, the following equations have to be solved:

$$\rho C\frac{d\theta}{dt} - \text{div}(\lambda.\mathbf{grad}\theta) - Q = 0 \quad \text{in} \quad \Omega \tag{19}$$

$$\lambda.\mathbf{grad}\theta.n = q(\theta,t) \quad \text{on } \partial\Omega_\theta \tag{20}$$

$$\theta = \theta_p(t) \quad \text{on } \partial\Omega_\theta \quad \text{with} \quad \partial\Omega = \partial\Omega_q \cup \partial\Omega_\theta \tag{21}$$

where θ, $\rho(\theta)$, $C(\theta)$, and $\lambda(\theta)$ are the temperature, the density, the specific heat, and the thermal conductivity, respectively, and Ω is a bounded domain (boundary $\partial\Omega$) representing all the conductive media.

Q represents the power losses through the Joule effect. The mean power over one period T of the source current is equal to $Q(\mathbf{x}) = 1/(\sigma T)\int_0^T \mathbf{J}^2(\mathbf{x},t)dt$. Considering the expression of $\mathbf{J}$ through a Fourier series, Q can be written as follows:

$$Q(\mathbf{x}) = \frac{1}{2\sigma(\theta)} \sum_{k=1,3}^{m} \left((\mathbf{J}_{kc}(\mathbf{x}))^2 + (\mathbf{J}_{ks}(\mathbf{x}))^2 \right). \tag{22}$$

IV. Direct Method

The finite-element approximation uses $m+2$ degrees of freedom at each node (m being the order of the highest harmonic considered), namely the temperature and the sine and cosine parts of the $(m+1)/2$ harmonics of the magnetic vector potential.

The application of the FEM then leads to the resolution of a system of $m+2$ coupled nonlinear equations for each node and at each thermal time step

$$\left\{ \begin{array}{c} \{\mathbf{R}_1(\{\theta\},\{A_{1c}\},\{A_{1s}\},\ldots)\} = 0 \\ \{\mathbf{R}_2(\{\theta\},\{A_{1c}\},\{A_{1s}\},\ldots)\} = 0 \\ \{\mathbf{R}_3(\{\theta\},\{A_{1c}\},\{A_{1s}\},\ldots)\} = 0 \\ \ldots \end{array} \right\}. \tag{23}$$

The first equation in (23) corresponds to the thermal problem. The $m+1$ other equations correspond to the finite-element formulation associated with (2) and (3). These equations are solved using the Newton-Raphson method. Iterations are performed until either the maximum absolute value of the nodal residual [see (23)] or the maximum variation of degrees of freedom between two successive iterations become less than prescribed thresholds. In our case, these thresholds are defined proportionally to the values obtained at the beginning of the iteration process using the coefficient $\epsilon = 10^{-2}$.

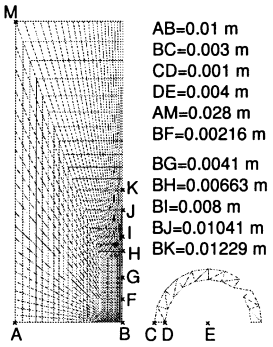

Fig. 1. Mesh of the device — steel part and inductor.

V. Application

We consider the heating of a steel piece using a static single-turn copper inductor. The simulation is performed under an axisymmetric assumption and, for symmetry reasons, only half of a meridian section is considered (Fig. 1). The whole mesh (component + inductor) includes 1340 elements and 1323 nodes. Air is not meshed and treated with boundary elements.

The electromagnetic properties of the component are temperature-dependent. The electric conductivity σ ($\Omega^{-1}.\text{m}^{-1}$) is defined as a piecewise linear function defined by a series of (θ,σ) values where the temperature is θ (°C). The following couples of values are used: $(0, 5.556*10^6)$, $(200, 3.333*10^6)$, $(400, 2.0 * 10^6)$, $(600, 1.282 * 10^6)$, $(800, 0.909 * 10^6)$, $(1000, 0.840*10^6)$, $(1200, 0.820*10^6)$, $(1400, 0.769*10^6)$, $(2000, 0.616*10^6)$. The magnetization curves are defined by the formula: $B(H,\theta) = (\mu_0 + (B_0(\theta)/(H+1273)))*H$ (B in Tesla and H in $\text{A}\cdot\text{m}^{-1}$) where $\mu_0 = 4\pi*10^{-7}\, H\cdot\text{m}^{-1}$ and the coefficient B_0 depends on the temperature. Temperature θ and coefficient B_0 are related by a piecewise linear function: (0,1.6), (200,1.588), (400,1.552), (500,1.522), (600,1.474), (650,1.432), (700,1.360), (735,1.240), (740,1.120), (745,1.0), (768,0.0). The following thermal properties have been considered: $\rho = 7800\ \text{kg}\cdot\text{m}^{-3}$, $C = 460\ \text{J}\cdot\text{kg}^{-1}\cdot\text{K}^{-1}$ and $\lambda = 30\,\text{W}\cdot\text{m}^{-1}\cdot\text{K}^{-1}$. For the inductor, $\sigma = 59*10^6\,\Omega^{-1}\cdot\text{m}^{-1}$, $\mu = \mu_0$, $\rho = 8930\,\text{kg}\cdot\text{m}^{-3}$, $C = 386\,\text{J}\cdot\text{kg}^{-1}\cdot\text{K}^{-1}$ and $\lambda = 400\,\text{W}\cdot\text{m}^{-1}\cdot\text{K}^{-1}$. A sinusoidal voltage $V_{1c} = 28$ V is applied to the inductor during 2.6 s and its frequency is equal to 50 kHz.

The finite-element software SYSWELD is used for all calculations. Two simulations are performed with the direct method considering only one harmonic for the first one and two harmonics for the other one. A third simulation has been performed with a staggered method considering a strong coupling between both phenomena and three periods of the source current. This simulation is considered as the reference because it fully accounts for all the nonlinear phenomena. For all simulations, the

	1) 1st order harmonic	2) 1st and 3rd order harmonics	3) staggered method
Solver	direct	direct	iterative
CPU Elapsed time	CP U = 1 687 0 h 40 min	CP U = 6 601 1 h 58 min	CP U = 17 290 7 h 02 min
Same computer for all simulations: PC PentiumIII 1Ghz RAM=512MO			

Fig. 2. Characteristics of the different simulations.

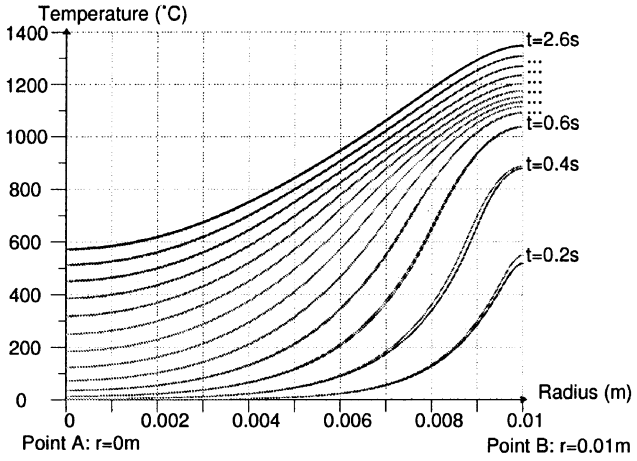

Fig. 3. Temperature profiles between A and B at different instants.

thermal time step is equal to $\Delta t_{\mathrm{ther}} = 0.1\ s$ and the accuracy associated with the Newton-Raphson solution procedure is the same for all. Fig. 2 summarizes the characteristics for all simulations that have been realized. Fig. 3 gives temperature profiles between nodes A and B (see Fig. 1) at different time steps from 0.2 to 2.6 s every 0.2 s for simulations 3 and 2. At the end of the process simulation, the temperature has reached a maximum of about 1347 °C in B and 571 °C in A (simulation 3). If now both profiles are subtracted, it is calculated that the maximum temperature difference is found maximum at node (0.0088,0.0) at time $t = 0.4\ s$. This quantity is equal to $+42\,^{\circ}\mathrm{C}$ and the temperature at this node is equal to 623 °C (simulation 3). It means that the maximum temperature difference between the staggered and direct (two harmonics) simulations is less than 7% (checked for all nodes at any time) whereas the total elapsed time is approximately reduced by a factor 3.5 with simulation 2. If now the same comparison is made for simulations 3 and 1, it leads to a very high maximum temperature difference equal to 30% at node (0.009 22,0.0), $t = 0.4\ s$, $\Delta\theta = +218\,^{\circ}\mathrm{C}$ and $\theta = 771\,^{\circ}\mathrm{C}$ (simulation 3).

In Fig. 4, the evolution of the temperature as a function of time, from $t = 0$ s till $t = 2.6$ s, is represented at different points of the heated surface i.e., B, F, G, H, I, J, and K. The curves highlight the fact that the properties of material are nonlinear. The comparison between simulations shows that, for the operating conditions of this simple example, the direct method with two harmonics gives quite accurate results compared to the reference. The advantage of the direct approach is that the total elapsed time is reduced in comparison with the staggered method which requires a lot of savings and readings on the physical disk of the computer.

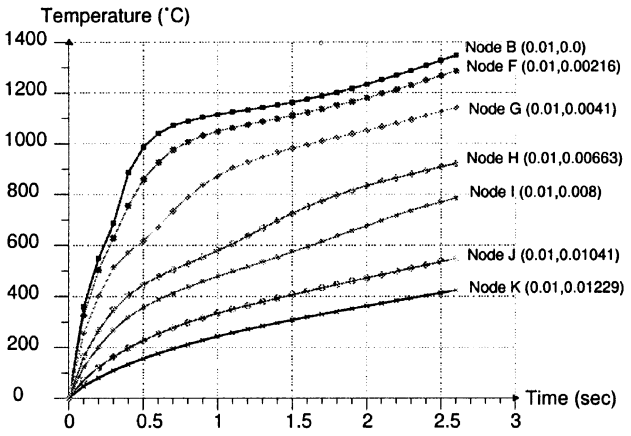

Fig. 4. Evolution of the temperature in differents nodes as a function of time.

VI. Conclusion

The paper presents only comparisons between numerical formulations as no experimental measurement concerning the example presented above is available. Comparisons with other numerical methods such as the one using a modified equivalent reluctivity is in progress. The presented results prove that the coupling between finite elements and boundary elements is successful when the harmonic balance method is associated with. Combined with the direct method which strongly couples magnetodynamic and thermal nonlinear problems, it represents an interesting tool for the numerical simulation of induction heating processes. The direct method is easier to use and is compatible with the use of boundary elements which avoids any meshing of air and simplifies the treatment of moving parts. It gives also accurate and faster results than a staggered method. It could be very simple to apply the direct method to an example including moving parts.

References

[1] M. Feliachi and G. Develey, "Magneto-thermal behavior finite element analysis for ferromagnetic materials in induction heating devics," *IEEE Trans. Magn.*, vol. 27, pp. 5235–5237, Nov. 1991.

[2] Y. D. Terrail, J. C. Sabonnadiere, P. Masse, and J. L. Coulomb, "Non-linear complex finite elements analysis of electromagnetic field in steady-state ac devices," *IEEE Trans. Magn.*, vol. MAG-20, pp. 549–552, July 1984.

[3] R. Pascal, J.-M. Bergheau, and P.Ph. Conraux, "Direct coupling between magneto-dynamic and thermal analysis allowed by a multi-harmonic decomposition of magnetic vector potential," in *Proc. 13th COMPUMAG*, vol. 3, July 2001, pp. 94–95.

[4] J. Lu, S. Yamada, and K. Bessho, "Time-periodic magnetic field analysis with saturation and hysteresis characteristics by harmonic balance finite element method," *IEEE Trans. Magn.*, vol. 26, pp. 995–998, Mar. 1990.

[5] R. Pascal, P. Conraux, and J.-M. Bergheau, "Numerical simulation of induction heating processes—comparison between direct multi-harmonic and classical staggered approaches," in *Proc. 7th Int. Conf. Advanced Computational Methods in Heat Transfer*, B. Sunden and C. A. Brebbia, Eds., Apr. 2002, pp. 393–403.

[6] J.-M. Bergheau and Ph. Conraux, "FEM-BEM coupling for the modeling of induction heating processes including moving parts," *J. Shanghai Jiaotong Univ.*, vol. E-5, pp. 91–99, June 2000.